Fizika Nizkikh Temperatur, 2007, v. 33, Nos. 6/7, p. 772–777

FTIR spectra and conformations of 2′-deoxyuridine in Kr matrices

A.Yu. Ivanov and V.A. Karachevtsev

B. Verkin Institute for Low Temperature Physics and Engineering of the National Academy of Sciences of Ukraine
47 Lenin Ave., Kharkov 61103, Ukraine
E-mail: ivanov@ilt.kharkov.ua

Received November 20, 2006

The Fourier transform infrared spectra in the range 4000–200 $см^{-1}$ of pyrimidine nucleoside 2′-deoxyuridine (dU) have been obtained in the low temperature inert Kr matrices. For the first time, instead of a usual flat mirror, a low temperature one-coordinate retroreflector was used as the matrix substrate. Owing to this, the matrix setup is insensitive to dip angle vibrations of the cryostat and is favourable to work with thinner matrix layers. Of two *syn*-conformers with dU_s1 and dU_s2 (stabilized by the intramolecular hydrogen bond O5′H…O2), only dT_s2 conformer with C2′-endo structure of the ribose ring was uniquely quenched. The height of the interconversion barrier of the minor *syn*-conformer dU_s1 was estimated to be below 0.7 kcal/mole. It was shown that the energy relaxation of impurities in Kr is slower than in Ar matrices.

PACS: **33.15.–e** Properties of molecules;
67.80.Cx Structure, lattice dynamics, and sound propagation.

Keywords: Fourier transform infrared spectra, matrix isolation, low temperature retroreflector, nucleoside.

Introduction

The structure and stability of molecular fragments of biomolecules in the gas phase, which are of great interest for understanding life on the molecular level, are investigated by different modern experimental methods [1], including such methods as He nanodroplets isolation (HENDI) [2,3], cavity ring-down spectroscopy (CRDS) [4,5], and conventional Fourier transform infrared (FTIR) spectroscopy. In spite of distinctions between these methods, cooling of preliminary evaporated molecules is common to these methods. Owing to fast cooling, the molecular structures may be fixed in the isolated state at low temperatures, but interconversion processes are observed between low barrier conformers [6,7]. Previously we used FTIR spectroscopy in inert matrices to investigate conformers of pyrimidine nucleosides [8–10]: 2`-deoxyuridine [9] and thymidine [10]. Three conformers with *anti*-orientation of the pyrimidine ring were found in Ar and Ne matrices [9,10], but among the two possible *syn*-conformations with intramolecular hydrogen bond O5′H…O2 (Fig. 1), only dU_s2 with C2′-endo conformation of 2′-deoxyribose ring were found in inert matrices. The transitions between C2′-endo and C3′-endo conformations of the sugar ring were subject of numerous

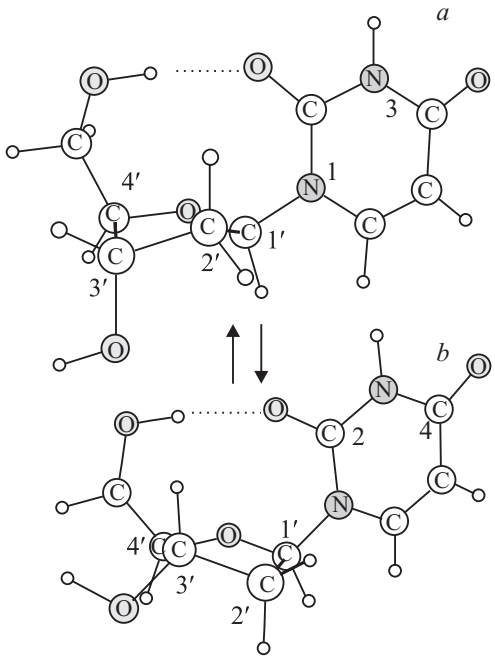

Fig. 1. The molecular structure and atom numbering of *syn*-conformations 2′-deoxyuridine: dU_s2 conformer with C2′-endo conformation of 2′-deoxyribose (*a*); dU_s1 conformer with C3′-endo conformation of 2′-deoxyribose (*b*). Intramolecular H-bonds O5′H—O2 are represented with dashed lines.

calculations and experiments [11–14]. The first calculation [11] was made by the method of molecular mechanics and the height of the barrier $\Delta E^{\#}$ between C2′-endo and C3′-endo conformations of 2′-deoxyribose was estimated to be 0.6 kcal/mole. In more recent molecular mechanics calculations with a stochastic difference equation algorithm [12], the value $\Delta E^{\#}$ = 2 kcal/mole was obtained. *Ab initio* calculations at the MP2/6-31G* level gave $\Delta E^{\#}$ 4 kcal/mole [13]. NMR studies of purine nucleosides in solutions showed this barrier to be 4.7 kcal/mole [14]. For this work we performed *ab initio* calculations at DFT and MP2 levels with correlated consistent basis sets as well as experiments in Kr matrices, using a more advanced experimental method.

Experimental and computational methods

Most of the important features of our matrix isolation setup have been described elsewhere [9,10,15,16]. Nucleosides are very thermally labile molecules and for their evaporation a special evaporation system with a short distance to the low temperature mirror and with reduced molecular beam losses was used [8–10] (Fig. 2). Furthermore, FTIR matrix isolation spectroscopy of nonplanar conformational-flexible molecules (like sugar, nucleosides, nucleotides…) encounters some additional problems. Such molecules have relatively broad spectral bands in FTIR spectra (5–10 cm^{-1} in comparison with 0.3–1 cm^{-1} in the spectra of nucleic acid bases, which have flat pyrimidine rings [15]) and the sensitivity of spectral experiments is lower. Consequently, thick matrix samples (thicker than 0.1–0.5 mm) must be prepared

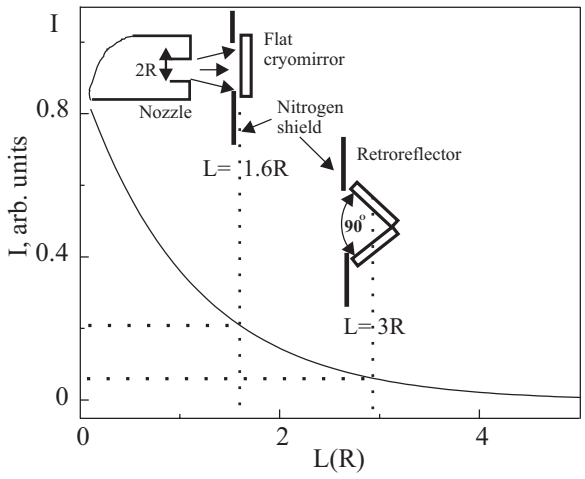

Fig. 2. The evaporation scheme with flat cryomirror and cryoretroreflector with the relationship of the intensity of molecular beam (*I*) as function of the distances *L* between the cell and cold substrate. *L* is in the unit of radius (*R*) of the outlet nozzle of cell. This scheme reflects actual distances of cryosubstrates *L*(*R*) from the nozzle of evaporation cell.

to improve sensitivity, jet thick matrices have poorer optical quality (especially in the short-wave region above 2000 cm^{-1}) and a tendency to mechanical collapse. For one, it is so for large guest molecules like 4-penthyl-4′cyanobiphenyl [17].

Previously, in order to improve the optical characteristics of Ar matrices, prior to matrix samples preparation, we deposed a thin layer of pure Ar on the cold mirrors over the temperature range of 35–20 K [16]. As the next step, in this investigation we, for the first time, used a retroreflector (functioning as an Amichi prism, Fig. 2). Owing to the additional reflection, the retroreflector permits work with thinner layers than those with a flat mirror. Unfortunately, the evaporation cell in this design has an expanding beam and a strong dependence of the molecular beam density on the distance between the cell and cryomirror (Fig. 2). Because of this design, the advantage in absorption band intensities was not realized. The unique peculiarity of the retroreflector is in that the tilt has no influence on the parallelism of the incoming and outcoming beams [18]. Therefore, the matrix setup with retroreflector is insensitive to the tilt . However, if there is a need to work at grazing angle there is a possibility to adjust the retroreflector so that work at grazing angles becomes feasible. It is well known that reflection at grazing angles [19] is necessary for efficient spectroscopy of thin films, for example, in surface enhanced infrared absorption (SEIRA) spectroscopy. With retroreflector, work at grazing angles can be peformed without an additional optical window in the vacuum chamber and without alignment of the additional spectrometer optics.

In this work, FTIR spectra of pyrimidine nucleoside 2′-deoxyuridine (dU) were obtained in low temperature inert Kr matrices in the range 4000–200 cm^{-1}. The low temperature differential quartz crystal microbalance (QCM) was used to measure absolute intensities of molecular beams and matrix-to-sample ratio (M/S) [15]. The M/S ratio was about 600:1 for all experiments in Kr matrices. Owing to QCM, we were able to work not only with Ar flux passing through the Knudsen cell but with extra flux of cold Ar gas also. The Kr gas was 99.99% pure, Kr matrices were deposited at the temperatures of the mirrors: namely, 9 K for the flat mirror, and 6 K for the retroreflector.

Experimental data were compared with *ab initio* calculations, which were performed by PC GAMESS version 7.0 [20] of GAMESS program [21]. Large part of calculations were performed on a dual AMD Athlon-MP workstation run in SMP mode. The stability of 2′-deoxyuridine conformers (Fig. 1) were estimated with correlated consistent basis cc-pvdz basis sets [22,23] within DFT/cc-pvdz and MP2/cc-pvdz. The DFT/cc-pvdz method was used for to calculate vibrational spectra and estimate the free Gibbs

energy G (harmonic oscillator-rigid rotor approximation) by using the standard capabilities of the PC-GAMESS.

Results and discussion

For conformations of nucleosides, the region of stretching (ν) vibrations νOH, νNH (3600–3400 cm^{-1}) is the most informative. As can be seen in Fig. 3, spectra of dU in Kr matrices are quite similar to those in Ar matrices [9], while all bands in Kr have low frequency shifts. The shape of the spectral lines of H-bonded νO5′H of dU_s2 conformer in Ar and Kr matrices does not differ significantly (Fig. 3). However, spectra in Kr matrix on the flat mirror at 9 K contain a new weak band at 3514 cm^{-1} (Fig. 3, curve *2*). The intensity of this band increased (Fig. 4) after a long infrared irradiation by the globar of the Fourier spectrometer in the range 400–4500 cm^{-1} (as determined by selective properties of KBr beamsplitter). It is significant that this IR-induced effect was not observed for dU conformers in Ar and Ne matrices [9]. IR-induced interconversions in the low temperature matrices are known for many compounds [24,25]. Similar to these data, the spectral changes can be explained by IR-induced conformational transition from dU_s2 to dU_s1 conformer with C3′-endo conformation of 2′-deoxyribose. According to DFT/cc-pvdz calculations of the vibrational spectra (Table 1) the 3514 cm^{-1} band may be assigned to H-bonded νO5′H of dU_s1 conformer (Fig. 1) as well.

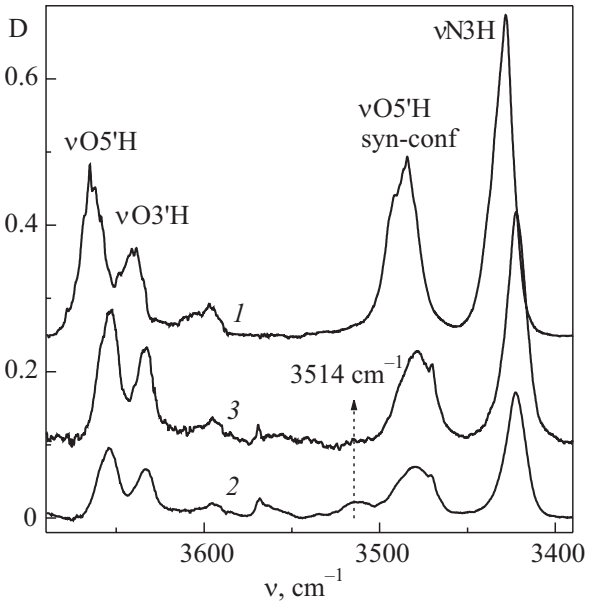

Fig. 3. The comparison of FTIR spectra of 2′-deoxyuridine in: Ar matrix at flat mirror (T = 5 K, M/S = 700) (*1*), Kr matrices at flat mirror (T = 9 K, M/S = 600) (*2*), Kr matrices at retroreflector (T = 6 K, M/S = 600) (*3*) in the O–H, N–H stretching region (3690–3390 cm^{-1}).

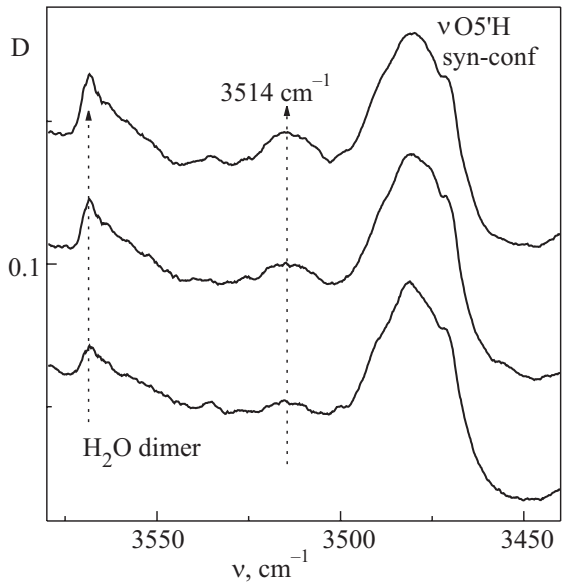

Fig. 4. The influence of globar irradiation on the water bands in Kr matrices with 2′-deoxyuridine (T = 9 K, M/S = 600.) The temporal interval — 30 min.

Table 1. The frequencies and intensities of experimental spectral bands in the FTIR spectra of 2′-deoxyuridine in Kr matrices and calculated ones (DFT/cc-pvdz) for dU_s1 and dU_s2 conformers

Conformer	Experiment		dU_s1*	dU_s1	dU_s2*	dU_s2
mode	ν, $см^{-1}$	I	ν, $см^{-1}$	I^a	ν, $см^{-1}$	I^a
νO5′H	3654	1.5				
νO3′H	3633	1	3644	36	3633	25
ν hb_O3′H	3580	0.5				
ν hb_O5′H	3615					
	3514	0.2				
ν hb_O5′	3480	1.6	3528	317	3482	507
νN3H	3422	2.5	3443	68	3444	72

Comment: I — relative integral intensities; I^a — absolute integral intensities [km/mol]; vhb_OH — bands of groups involved in the intramolecular H-bonds. * — Scaling factor for calculated frequencies = 0.962.

But furthermore, it was found that the intensity of this band is not well reproducable. As shown in Fig. 3, the 3514 cm^{-1} band in Kr on the retroreflector at 6 K (Fig. 3, curve *3*) is practically absent. It was so in some experiments with a flat mirror as well. To explain this discrepancy, we focused our attention on the spectral behavior of a water impurity. The weak donor band of a water dimer at 3568.7 cm^{-1} [26] is present in the dU spectra in Kr matrices (Fig. 3,4). Under IR-irradiation this band increased in intensity together with the 3514 cm^{-1} band (Fig. 4). In additional, according to Engdall and Nelander [26], the water trimer band is also at 3514.2 cm^{-1}. As a rule, a small

amount of H_2O molecules can be trapped in the matrix at a quickened performance of experiment. Nevertheless, water dimers in Ar matrices (and especially trimers) did not practically form and did not interfere with experiment (Fig. 5). For a more sophisticated solution of this problem, as before [9], we used UV irradiation to shift the conformational equilibrium of dU. The UV-induced interconversion and some decomposition were previously observed for dU samples in Ar matrices [9]. In comparison with that work, a pronounced UV decomposition of dU in Kr matrices was obvious (Fig. 6). Unlike experiments in Ar matrices [9], the UV decomposition in Kr was accompanied by an increase of the intensities of the 3568 cm^{-1} and 3514 cm^{-1} spectral bands (Fig. 6) and of the water monomer bands in the region 3800–3650 cm^{-1} (not displayed). It should be also noted that, owing to thinner matrices the efficiency of UV irradiation of the matrix samples on retroreflector was somewhat higher than on flat mirror.

These results correlate with the known data for the efficiency of photoprocesses in different matrix media. As a rule, the quantum yield of photoisomerization decreases in the sequence Xe, Kr, Ar, N_2 [24,25]. Previously, we observed a drop in the efficiency of the UV-induced interconversion of glycine conformers in Kr, Ar, Ne [9]. These results may be in part explained by the influence of the size of the matrix cage, since the heavier gases with a larger cage interact weaker with impurity molecules [25]. Hence, the stronger UV decomposition of dU in Kr, as compared to Ar, and the formation of water dimers might be caused by slower energy relaxation from impurity to

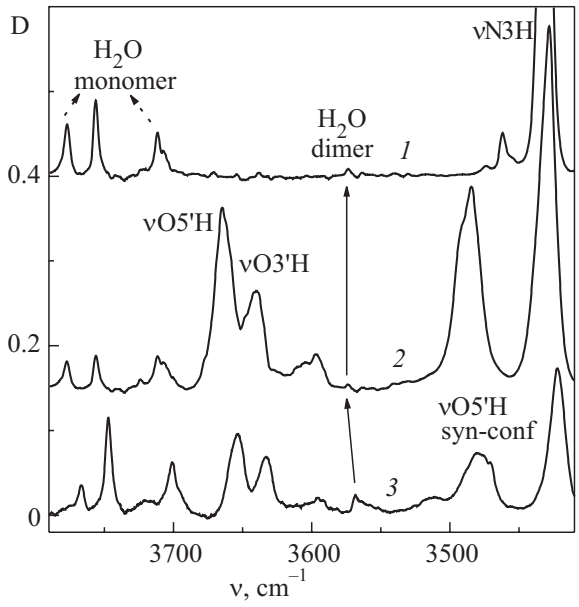

Fig. 5. The manifestation of water impurity bands in the different matrices: Ar matrix with 1-methyluracil (T = 11 K) (*1*), Ar matrix with 2′-deoxyuridine (T = 11 K) (*2*), Kr matrices at flat mirror (T = 9 K) (*3*).

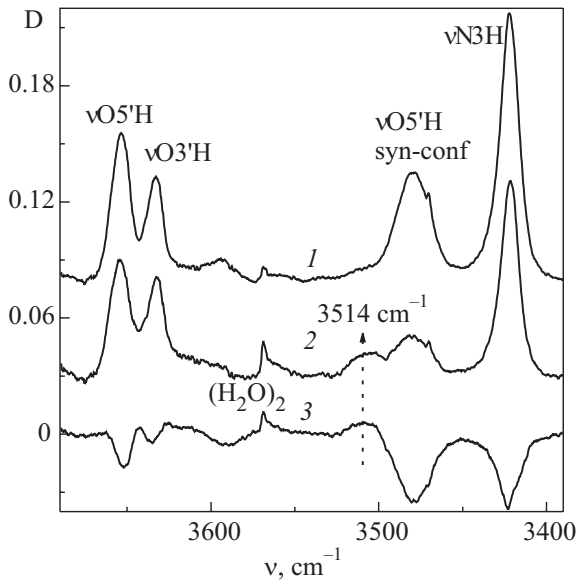

Fig. 6. Effect of UV irradiation on the FTIR of spectrum of 2′-deoxyuridine isolated in Kr matrix (T = 6 K, M/S = 600) in the O–H, N–H stretching region (3690–3390 cm^{-1}): spectrum before UV irradiation (*1*); spectrum after UV irradiation (*2*); difference spectrum after UV irradiation (t = 20 min) (*3*).

the matrix. However, the results of Fig. 4 cannot be explained by the cage effect. As can be seen in Fig. 4, despite more stronger interaction between the Kr atom and the water molecule, water dimers and trimers formed more effectively on the surface of Kr matrices than Ar ones. This process is not practically affected by cage dimentios. Obviously, water impurities have longer relaxation times and longer diffusion paths on the Kr surface than with Ar. It is interesting to note in this connection the result of Reva *et al.* [27] who demonstrated depletion of the low-barrier (~0.7 kcal/mole) cyanoacetic acid gauche conformers in the sequence of matrices Xe, Kr, Ar. It can be therefore inferred that relaxation on the surface of matrices plays an important role in depopulation of the low-barrier conformers.

To understand the above problems qualitatively, simplified transition kinetics between dU_s1 and dU_s2 conformers of dU was considered. The energy relaxation profile along the dihedral angle C1′C2′C3′C4′ (or ν3, according to [11]) is shown in Fig. 7. It was assumed that the transition takes place in the framework of *syn*-conformation, without breaking H-bond O5′H–O2. The position of the pyrimidine ring is important since the C2O group may influence the position of O4′ in the ribose ring and, hence, the barrier height. Therefore, our results (Fig. 7) are noticeably distinct from calculations by Foloppe and MacKerell [12] for model compounds of 2′-deoxyribose. In our calculations the barrier height of transition dU_s1 and dU_s2 is about 0.7 kcal/mole at DFT level and 1.3 kcal/mole at MP2 level (Fig. 7).

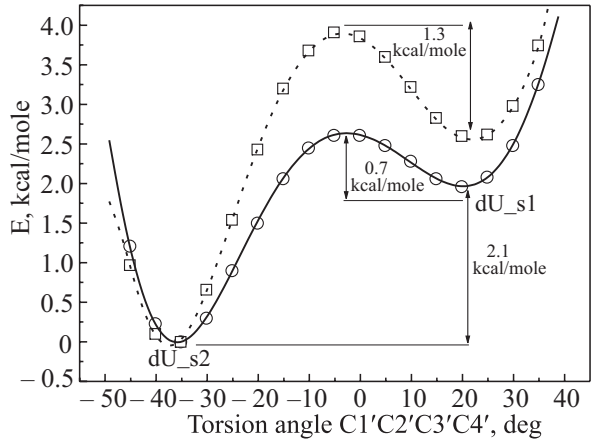

Fig. 7. The energy relaxation profile between dU_s2 and dU_s1 conformers along dihedral angle C1′C2′C3′C4′ calculated by the methods DFT/cc-pvdz (circles) and MP2/cc-pvdz (squares).

According to the conventional transition state theory (TST), the classical rate constants K_{TST} can be estimated from the Eyring equation [28]:

$$K_{TST} = \frac{k_B T}{h} e^{-\Delta G^{\#}/RT}, \quad (1)$$

where $\Delta G^{\#}$ is the free energy of the barrier, h and k_B are the Planck and Boltzmann constants.

Similarly as was done by Jensen and Gordon for glycine [28], the Wigner correction for quantum tunneling effects is:

$$K^{w}_{TST} = K_{TST}\left[1+\frac{1}{24}\left(\frac{h\nu}{k_B T}\right)^2\left(1+\frac{RT}{\Delta G^{\#}}\right)\right], \quad (2)$$

where the imaginary frequency at the saddle point is denoted by ν. Assuming that only one-way transitions occur, the number of molecules dN which passed through the barrier during dt is:

$$dN = -K^{w}_{TST} N dt \quad (3)$$

Integration of Eq. (3) with the initial number of molecules N_0 leads to:

$$N(t) = N_0 e^{-K^{w}_{TST} t}. \quad (4)$$

The time of transition of one-half of molecules $T_{1/2}$ from one conformer to another has the form

$$T_{1/2} = \frac{\ln 2}{K^{w}_{TST}} = \frac{0.693}{K^{w}_{TST}}. \quad (5)$$

Obviously, depopulation of the low-barrier conformer (or, in other words, «conformational cooling» [6,27]) will occur if the energy relaxation time is close to $T_{1/2}$. The results of calculations using Eqs. (1)–(5) for different temperatures and barriers heights are summarized in Table 2. One can see that, by extrapolations the reported experimental data [7,27], the conformers with barriers of about 0.7 kcal/mole can be easily conserved in the isolated state at 6 K. But it is possible only if the energy relaxation is very fast, otherwise, the population of conformers will change.

Table 2. The time (s) of $T_{1/2}$ of transition of one-half number of molecules from the one conformer to another calculated by Eqs. (1)–(5) (the reverse transition was ignored)

Barrier, kcal/mole	The time (s) of $T_{1/2}$ of transition for different temperature (K)				
	430 K	300 K	200 K	12 K	6 K
0.3	$1.1\cdot10^{-13}$	$1.9\cdot10^{-13}$	$3.7\cdot10^{-13}$	$1.2\cdot10^{-6}$	9.0
0.7	$1.7\cdot10^{-13}$	$3.5\cdot10^{-13}$	10^{-12}	9.9	$2.5\cdot10^{13}$
1.3	$3.4\cdot10^{-13}$	10^{-12}	$4.6\cdot10^{-12}$	$8\cdot10^{11}$	$>2.5\cdot10^{13}$
2.0	$8\cdot10^{-13}$	$3\cdot10^{-12}$	$2.5\cdot10^{-11}$	$>8\cdot10^{11}$	$>2.5\cdot10^{13}$
3.0	$2.6\cdot10^{-12}$	$1.7\cdot10^{-11}$	$3\cdot10^{-10}$	$>8\cdot10^{11}$	$>2.5\cdot10^{13}$

Among the above-mentioned methods (HENDI, CRDS, and matrix isolation), the process of cooling is the longest in CRDS, which used seeded molecular beams, since gas-dynamic cooling occurs due to numerous collisions in the supersonic part of nozzle [29]. The supersonic cooling typically quenches the population of conformers if the barrier exceeds 1 kcal/mole [30]. In addition, the carrier gas and the backing pressure influence this process. As was shown by Ruoff *et al*. [30], the «conformational cooling» increase in the sequence He, Ar, Kr, Xe. From the gas-dynamic investigations [31] it is known that the energy thermal accommodation coefficient decreases in the reverse sequence of these atoms. Because of this, a small coefficient of accommodation is to be compensated by higher frequency of collisions.

The faster energy relaxation and, consequently, the effecient «conformational quenching» may result in a direct contact of impurity molecules with superfluid helium nanodroplets in HENDI [32] or with the surface of low temperature matrices. As noted by Poliakoff and Turner [33], the energy relaxation rate is subject to variations directly as frequencies of the phonon spectrum. The frequencies of the phonon spectrum increase in the sequence of matrices — Xe, Kr, Ar [34]. It is interesting that the phonon spectrum of solid Ne is between those of Kr and Ar (Fig. 20.8 in [34]). These facts interpret in general the above-discussed data for photoisomerization of dU conformers and behavior of water impurity. At the same time, despite a relatively high barrier (Fig. 7), no reliable evidence of dU_s1 «conformational quenching» in Ar or Kr matrices was found. It may be due to two different factors. Firstly, the actual barrier height may be significantly lower than calculated (Fig. 7). Secondly, the cooling rate

of endocyclic torsion vibrations of dU_s1 may be relatively slow resulting in «conformational cooling». Using molecular matrices is likely to remove the first factor. As discussed by Poliakoff and Turner [33], these matrices can support additional channels of energy relaxation of impurities via vibrations of host molecules.

Conclusions

The conformational equilibrium of dU conformers with intramolecular hydrogen bonds in Kr matrices at 6–9 K is close to the observed equilibrium in Ne and Ar matrices at 5–30 K [9]. Basically, it may be thought that comparison with the gas phase is true also, with one exception for dU_s1 conformer with C3′-endo conformation of the ribose ring. The 3514 cm^{-1} band was assigned to the water trimer, but its overlap with H-bonded νO5′H of dU_s1 conformer is not completely excluded. For a reliable «conformational quenching» of dU_s1, use the H_2 or N_2 molecular matrices at lower temperatures (< 4 K) might be helpful.

It has been shown that a retroreflector enables work with thin Ar matrices, correlation with the evaporation system of thermally labile biomolecules, and improves the optical stability of the cryogenic matrix isolation setup. It is important that the retroreflector simplifies measurements at grazing angles and consequently enables investigations of very thin matrices. Use of the retroreflector scheme for surface enhanced infrared absorption (SEIRA) spectroscopy at low temperatures is promising for further investigation.

This investigation was supported by the National Academy of Sciences of Ukraine.

1. R. Weinkauf, J.-P. Schermann, M.S. de Vries, and K. Kleinermanns, *Eur. Phys. J*. **D20** 309 (2002).
2. S. Goyal, D.L. Schutt, and G. Scoles, *Phys. Rev. Lett*. **69**, 933 (1992).
3. M. Hartmann, R.E. Miller, J.P. Toennis, and A. Vilesov, *Phys. Rev. Lett*. **75**, 1566 (1995).
4. A. O'Keefe and D.A.G. Deacon, *Rev. Sci. Instrum*. **59**, 2544 (1988).
5. R.N. Casaes, J.B. Paul, R.P. McLaughlin, R.J. Saykally, and T. van Mourik, *J. Phys. Chem*. **A108**, 10989 (2004).
6. P. Felder and Hs.H. Gunthard, *Chem. Phys*. **71**, 9 (1982).
7. A.J. Barnes, *J. Mol. Struct*. **113**, 161 (1984).
8. S.A. Krasnokutski, A.Yu. Ivanov, V. Izvekov, G.G. Sheina, and Yu.P. Blagoi, *J. Mol. Struct*. **482–483**, 249 (1998).
9. A.Yu. Ivanov, S.A. Krasnokutski, G.G. Sheina, and Yu.P. Blagoi, *Spectrochim. Acta* **A59**, 1959 (2003).
10. A.Yu. Ivanov, S.A. Krasnokutski, and G.G. Sheina, *Fiz. Nizk. Temp*. **29**, 1065 (2003) [*Low Temp. Phys*. **29**, 809 (2003)].
11. M. Levitt and A. Warshel, *J. Am. Chem. Soc*. **100**, 2607 (1978).
12. N. Foloppe and J.A.D. MacKerell, *J. Phys. Chem.* **B102**, 6669 (1998).
13. K. Arora and T. Schlick, *Chem. Phys. Let.* **378**, 1 (2003).
14. W. Saenger, *Principles of Nucleic Acid Structure*, Springer Verlag, New York (1984).
15. A.Yu. Ivanov, A.M. Plokhotnichenko, E.D. Radchenko, G.G. Sheina, and Yu.P. Blagoi, *J. Mol. Struct.* **372**, 91 (1995).
16. A.Yu. Ivanov, G.G. Sheina, and Yu.P. Blagoi, *Spectrochim. Acta* **A55**, 219 (1999).
17. A.V. Vlasov, T.I. Shabatina, A.Yu. Ivanov, G.G. Sheina, A.V. Nemukhin, and G.B. Sergeev, *Mendeleev Commun.* **15**, 10 (2005).
18. R.J. Bell, *Introductory Fourier Transform Spectroscopy*, Academic Press (1972).
19. R.G. Greenler, *J. Chem. Phys*. **50**, 1963 (1969).
20. Alex.A. Granovsky, *http://classic.chem.msu.su/gran/gamess/index.html*.
21. M.W. Schmidt, K.K. Baldridge, J.A. Boatz, S.T. Elbert, M.S. Gordon, J.J. Jensen, S. Koseki, N. Matsunaga, K.A. Nguyen, S. Su, T.L. Windus, M. Dupuis, and J.A. Montgomery, *J. Comput. Chem*. **14**, 1347 (1993).
22. T.H. Dunning, Jr., *J. Chem. Phys.* **90**, 1007 (1989).
23. Basis sets were obtained from the Extensible Computational Chemistry Environment Basis Set Database, Version 02/25/04, (*http://www.emsl.pnl.gov/forms/basisform.html*) as developed and distributed by the Molecular Science Computing Facility, Environmental and Molecular Sciences Laboratory which is part of the Pacific Northwest Laboratory, P.O. Box 999, Richland, Washington 99352, USA, and funded by the U.S. Department of Energy.
24. T. Lotta, J. Murto, M. Rasanen, A. Aspiala, and P. Sarkka, *J. Chem. Phys*. **82**, 1363 (1985).
25. A.K. Knudsen and G.C. Pimentel, *J. Phys. Chem.* **95**, 2823 (1991).
26. A. Engdall and B. Nelander, *J. Mol. Struct*. **193**, 101 (1989).
27. I.D. Reva, S.G. Stepanian, L. Adamowicz, and R. Fausto, *Chem. Phys. Lett*. **374**, 631 (2003).
28. J.H. Jensen and M.S. Gordon, *J. Am. Chem. Soc*. **113**, 7917 (1991).
29. D.I. Kataev and A.A. Maltsev, *J. Exp. Theor. Phys*. **5**, 1527 (1973).
30. R.S. Ruoff, T.D. Klots, T. Emilsson, and H.S. Gutowsky, *J. Chem. Phys*. **93**, 3142 (1990).
31 F.O. Goodman and H.Y. Wachman, *Dynamics of Gas-Surface Scattering*, Academic Press, New York (1976).
32. C. Callegari, K.K. Lehmann, R. Schmied, and G. Scoles, *J. Chem. Phys*. **115**, 10090 (2001).
33. M. Poliakoff and J.J. Turner, in: *Chemichal and Biochemical Applications of Lasers*, C. Bradley Moor (ed.), Academic Press, New York (1980).
34. *Cryocrystals*, B.I. Verkin and A.F. Prihotko (eds.), Naukova Dumka, Kiev (1983) (in Russian).